Nearly frictionless faulting by unclamping in long-term interaction models

Tom Parsons U.S. Geological Survey, MS-999, 345 Middlefield Road, Menlo Park, California 94025, USA

ABSTRACT

In defiance of direct rock-friction observations, some transform faults appear to slide with little resistance. In this paper finite element models are used to show how strain energy is minimized by interacting faults that can cause long-term reduction in fault-normal stresses (unclamping). A model fault contained within a sheared elastic medium concentrates stress at its end points with increasing slip. If accommodating structures free up the ends, then the fault responds by rotating, lengthening, and unclamping. This concept is illustrated by a comparison between simple strike-slip faulting and a mid-ocean-ridge model with the same total transform length; calculations show that the more complex system unclamps the transforms and operates at lower energy. In another example, the overlapping San Andreas fault system in the San Francisco Bay region is modeled; this system is complicated by junctions and stepovers. A finite element model indicates that the normal stress along parts of the faults could be reduced to hydrostatic levels after ~60–100 k.y. of system-wide slip. If this process occurs in the earth, then parts of major transform fault zones could appear nearly frictionless.

Keywords: friction, faulting, San Andreas, transforms.

INTRODUCTION

Some faults exhibit very low shear strength and appear to resist sliding less than the rocks they are made of (e.g., Sibson, 1994). Perhaps the best-studied example is the San Andreas fault in California. If the fault interface has a typical coefficient of friction for rocks ($\mu \approx 0.6$–0.85) (Byerlee, 1978), then long-term slip should have produced a heat-flow anomaly that is not observed (e.g., Brune et al., 1969; Lachenbruch and Sass, 1980). Supporting observations include fault-orthogonal orientation of maximum horizontal stress (e.g., Zoback et al., 1987), and microseismicity triggered by shear stress changes (e.g., Reasenberg and Simpson, 1992). These observations are best fit with static friction coefficients of $\mu \approx 0.1$–0.2. Modeling studies that reconstruct fault slip and stress orientations are also best fit with low friction (e.g., Bird and Kong, 1994; Geist and Andrews, 2000).

The problem can be framed in terms of Coulomb failure $|\bar{\tau}_f| = \mu(\sigma_n - p) + C$, such that shear stress on a fault ($\bar{\tau}_f$) is balanced by frictional resistance that depends on fault-normal stress (σ_n), pore-fluid pressure (p), the friction coefficient (μ), and cohesion (C). When the shear stress term exceeds the frictional term, slip occurs. Observations that support the low-shear-strength faulting interpretation are blind to which components of the frictional term are responsible. Thus explanations of low-strength faulting have tended to appeal either to weak fault materials such that μ is very low, or high pore-fluid pressure such that the effective normal stress is low.

The most accepted suite of models for weak faults can be summarized as various means of sealing and overpressuring fluids within impermeable fault gouge (e.g., Byerlee, 1990; Rice, 1992; Sleep and Blanpied, 1992; Lockner and Byerlee, 1995; Miller et al., 1996). These models depend also on the complex interaction between fluids, fault-zone materials, and the stress field (e.g., Marone et al., 1990; Chester et al., 1993; Lockner and Byerlee, 1993; Wintsch et al., 1995; Moore et al., 1996; Saffer et al., 2001). However, questions remain concerning how overpressured fluids can be trapped within fault zones without release by hydrofracturing (e.g., Scholz, 1996). In this study I propose a contributing weakening process, i.e., the reduction of fault-normal stress caused by long-term interactions with other faults.

CONCEPT

Slip on an isolated fault of finite length concentrates stress at its terminations. Consider a sheared elastic solid containing a vertical, frictional fault. With increasing applied shear, the model fault slips, reducing stress along it. However, at the fault terminations stresses are increased and stored as elastic dilatation and contraction, evident as vertical deformation in the model (Fig. 1A). Without release, elastic strain concentrations make it increasingly difficult for the fault to move.

If accommodating structures exist at fault terminations, then a different result is obtained. For example, if passive spreading centers are added to the conceptual model (Fig. 1B), transform faults respond by deflecting slightly clockwise relative to the right-lateral shear direction (Fig. 2). Deflection occurs because fault terminations are less restricted; faults may lengthen and can interact with the spreading centers and other transforms. Fault interactions are often considered when

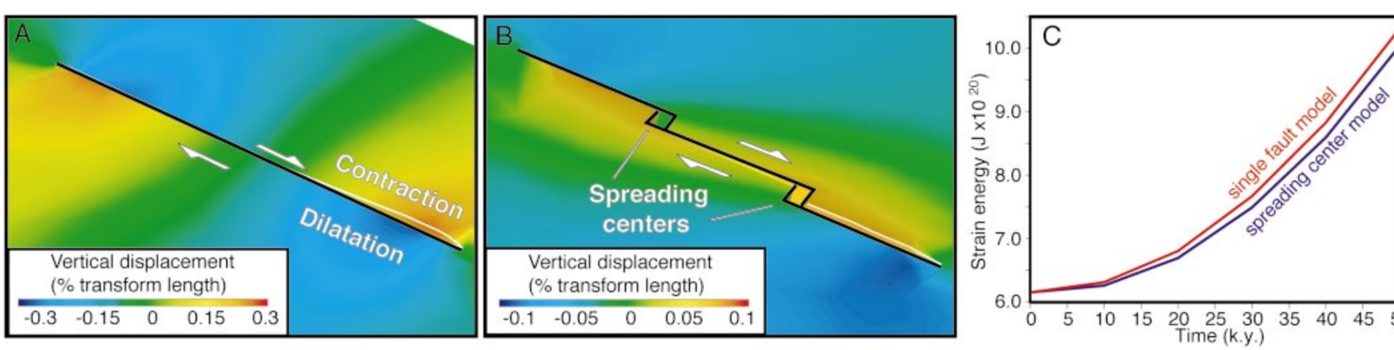

Figure 1. Deformation (scaled by factor 5 for easier viewing) and strain energy of faulting. A: Elastic finite element model of simple right-lateral strike-slip fault showing deformation and shaded contours of vertical displacement. Fault zones are allowed to deform continuously with increasing slip. B: Introduction of two spreading centers interrupting fault significantly reduces elastic strain concentrations, distributing deformation throughout model. C: Stored elastic strain energy is less in spreading-center model.

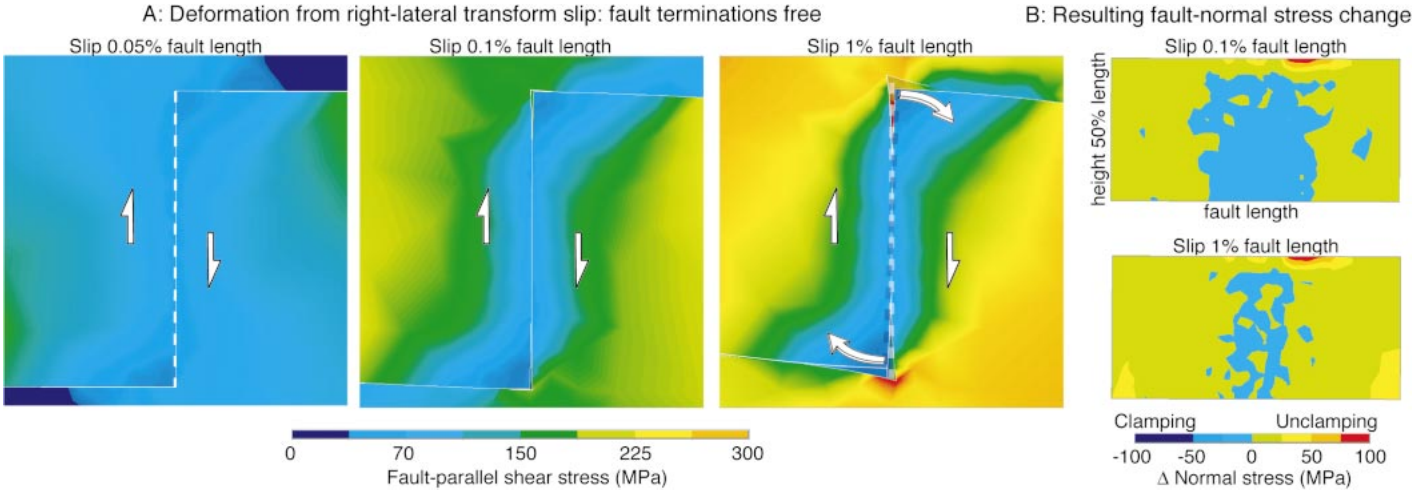

Figure 2. Map view of deformed shape (scaled by factor 10) and shear stress around transform fault intervening between two passive spreading centers. A: With increasing slip, walls of fault deflect as result of stress concentrations at fault terminations. Deflections result in slight clockwise rotation of right-lateral strike-slip fault and (B) unclamping.

modeling coseismic stress transfer from individual earthquakes (e.g., Harris, 1998); in this example, the longer term effect of spreading-center extension and slip on adjacent transforms is modeled (transforms slip ~3% of their length in 50 k.y.). The resulting deformation of transform faults includes opening, or unclamping (Fig. 2). A persistent reduction in normal stress acting across a fault enables it to slip more freely (e.g., Chester and Chester, 2000).

The two cases compared in Figure 1 show how a fault might interact with the surrounding crust and associated faults to reduce the normal stress component and thus the apparent friction. Movement is more difficult along a single fault with typical rock friction than along a system of shorter, interacting segments that have less normal stress acting across them. Comparison of the calculated strain energy of these two systems shows that the spreading-center model stores less elastic energy for the same amount of applied work (Fig. 1C).

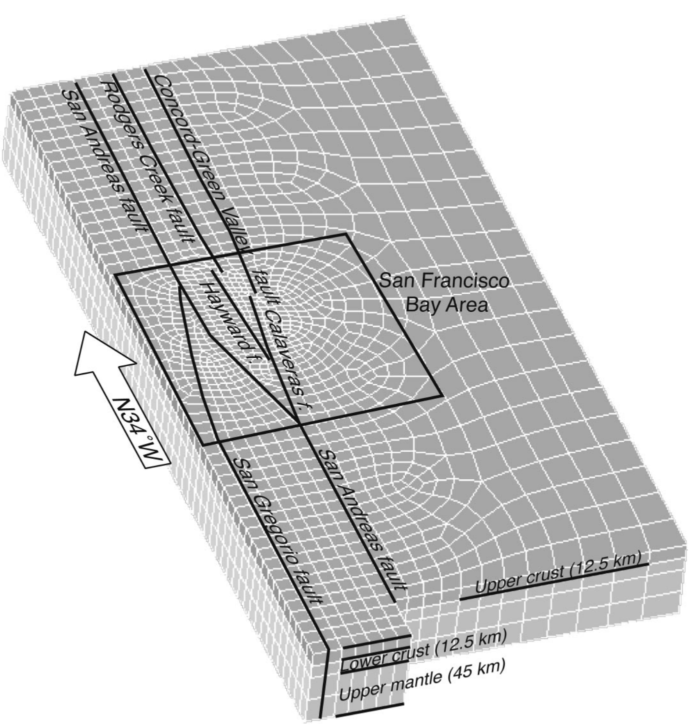

Figure 3. San Francisco Bay area finite element mesh and fault structures. Through-going vertical faults are discontinuities in model and have deformable contact elements on their surfaces that obey Coulomb failure criterion.

SAN ANDREAS SYSTEM IN THE SAN FRANCISCO BAY REGION

To examine the effects of long-term interactions on the stress state of a strike-slip fault system, a finite element model of the San Francisco Bay region was built. The model has three compositional layers inferred from measured crustal velocity structure (e.g., Holbrook et al., 1996; Hole et al., 2000). The upper 12.5 km of the model are crustal rocks approximated by wet Westerly granite (Hansen and Carter, 1983). The 12.5-km-thick lower crust has elastic properties representative of basalt-diabase composition (Caristan, 1982; Brocher et al., 1994). The 45-km-thick upper mantle layer is required to maintain isostatic balance with the crustal column at sea level (Lachenbruch and Morgan, 1990), and has properties associated with a combination of wet and dry dunite samples (Carter and Tsenn, 1987). The model edges are oriented parallel and orthogonal to the Pacific plate–Sierra Nevada block relative motion vector of ~N34°W (Fig. 3). Fault slip is induced by moving the western model edge at a rate of 39 mm/yr (e.g., De Mets et al., 1994; Savage et al., 1999). The eastern model edge is held fixed to North America, and is not free to move laterally. The model base is freely slipping laterally, but cannot move vertically.

The model is composed entirely of 8 node viscoelastic elements. The proportion of viscous to elastic behavior of a given element node is governed by the local crustal geotherm derived from heat-flow measurements (C. Williams, 2001, personal commun.). Temperature dependence of strain rate ($\dot{\epsilon}$) in the model is controlled by the creep equation $\dot{\epsilon} = A\exp(-Q_c/RT)\sigma^n$ (e.g., Kirby and Kronenberg, 1987), where A, Q_c (activation energy), and n are experimentally derived elastic constants, R is the universal gas constant, T is temperature, and σ is differential stress. In the lower temperature upper crust, the model behaves elastically, while deeper, higher temperature regions behave increasingly more viscoelastically.

The finite element model has cuts through the crust (e.g., Holbrook et al., 1996; Henstock et al., 1997; Parsons and Hart, 1999) that represent the major strike-slip faults of the San Francisco Bay region. The faults are deformable, and are constructed from contact elements that obey the Coulomb failure relation. Contact elements have zero thickness and are welded to the sides of viscoelastic elements. An

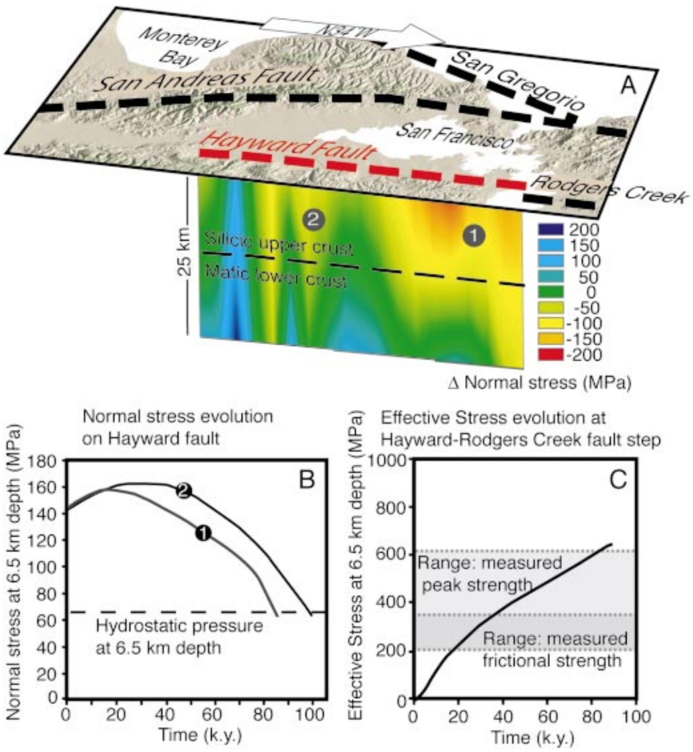

Figure 4. Normal stress change on Hayward fault after 100 k.y. of plate boundary motion. A: Areas of fault where normal stress was decreased (unclamping) are shown in tones of yellow and red. Zones of normal stress increase are shown in blue tones. Much of northern half of fault plane is unclamped. B: Normal stress history is plotted for two example points from fault plane. By ~85–100 k.y., normal stress at these two points has been reduced to hydrostatic levels. C: Modeled growth of effective stress 6.5 km deep in stepover between Hayward and Rodgers Creek faults is shown superimposed on measured range of frictional and peak strength of near-Hayward fault rocks (Morrow and Lockner, 2001). Failure in stepover is expected after ~20–60 k.y. of strike-slip deformation.

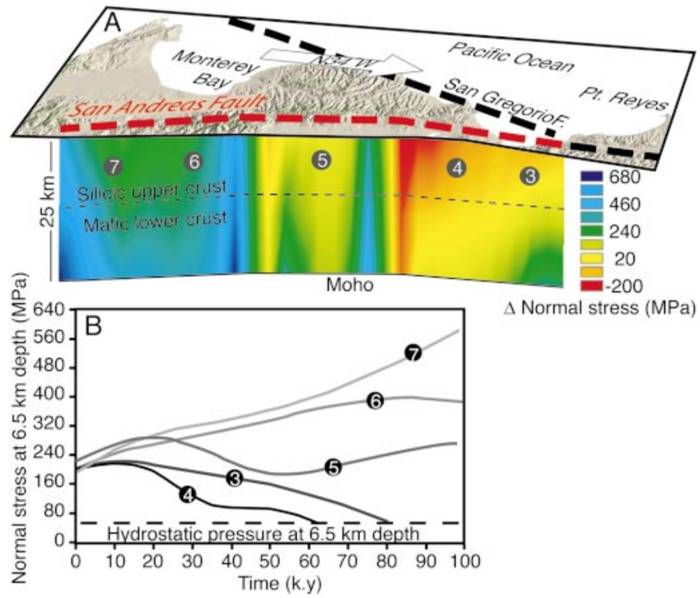

Figure 5. A: Normal stress change on Peninsular San Andreas fault after 100 k.y. of plate boundary motion. B: After ~60–80 k.y., normal stress at points to north has been reduced to hydrostatic. However, to south where there is restraining bend, normal stress increased with time.

important model assumption is that fault stepover zones are treated as discontinuities all the way through the model to depth. Fault friction coefficients were set at a relatively low value of $\mu = 0.4$, under the assumption that fault gouge and trapped pore fluids reduce friction. A similar model was used by Parsons (2002) to calculate tectonic stressing rates for earthquake-probability calculations; in that effort, the model reproduced long-term fault slip rates and shorter-term geodetic observations.

The Pacific plate was moved past the Sierra Nevada block at 39 mm/yr for a model 100 k.y. span to simulate long-term slip on the San Andreas fault system. Shear and normal stress components on the San Andreas and Hayward faults were tracked with time. The faults were allowed to slip according to the Coulomb criterion. The results from finite element modeling allow an image of the possible change in fault-normal stress over time on a complex set of interacting faults such as in the San Francisco Bay area.

Results From San Francisco Bay Area Simulation

Finite element modeling shows variable change in the normal stress with time along San Francisco Bay area faults. The modeled Hayward fault, for example, is unclamped along its north half because of a releasing step with the Rodgers Creek fault (Fig. 4). That fault configuration causes long-term interaction, such that slip on the southern Rodgers Creek fault reduces the normal stress across the north Hayward fault. A history of normal stress change is shown in Figure 4 for two points on the fault surface at 6.5 km depth. The plots show that after 85–100 k.y. of slip throughout the fault system, the normal stress on parts of the Hayward fault plane was reduced to hydrostatic levels. The required time would be less if fault zone fluids were overpressured. When normal stress is reduced to hydrostatic, a fault governed by Coulomb failure would behave almost as a frictionless surface, needing only to overcome cohesion to fail.

A model consequence of the right-stepping geometry between the Hayward and Rodgers Creek faults is stretching of the crust intervening between them. The finite element model predicts extensional failure in the stepover after ~20–60 k.y. of Hayward–Rodgers Creek fault slip (Fig. 4C). The trends of normal stress reduction (Fig. 4B) could change if faulting occurred in the stepover. However, the analogous spreading center transform models shown in Figures 1 and 2 indicate that interaction with extensional structures may also contribute to normal stress reduction.

Compared to the Hayward fault, a model of the Peninsular San Andreas fault shows more complexity in normal stress change with time because the Peninsular San Andreas fault bends relative to the plate motion vector (Fig. 5). The model indicates continuously rising normal stress across the fault to the south, where it makes a restraining bend (Fig. 5). North of the restraining bend, the fault is unclamped by varying degrees because of interaction with the adjacent San Gregorio fault; some points along the fault are reduced to hydrostatic after 60–80 k.y. of slip. The modeled variation in normal stress with fault orientation is consistent with observations of increased fault strength and complexity at restraining bends (Saucier et al., 1992; Scholz, 2000; Zoback, 2000). As in the Hayward fault example, there is rough correspondence between local topography and the normal stress state on the fault. There is high-standing compressional topography where normal stress rises with time, and the fault is below sea level where normal stress diminishes with time (Fig. 5).

The finite element model indicates that in a complex fault system with interacting branches, bends, and stepover zones, long-term slip on all segments may act to unclamp parts of the fault system. Although interaction leading to unclamping reduces frictional resistance on specific faults, it does not reduce friction in the system as a whole. Rather, frictional resistance of the major strike-slip faults is transferred into broad crustal deformation. A significant amount of the normal stress reduction could be stored as elastic strain in the rocks adjacent to the fault zones. For example, measured frictional strengths of Hayward fault zone rocks range between 200 and 300 MPa differential stress at mid-crustal depths (Morrow and Lockner, 2001), giving them ample strength to absorb the modeled unclamping along the north Hayward fault (Fig. 4), even if they are highly fractured.

CONCLUSION

Some model fault systems can cause long-term unclamping as a result of their geometry and ability to interact. Systems that can unclamp themselves, such as modeled mid-ocean-ridge transforms, are calculated to be energetically more favorable than one isolated fault. A finite element model of San Francisco Bay area faults indicates that the normal stress acting across parts of the Hayward and San Andreas faults can be reduced to hydrostatic levels after 60–100 k.y. of relative Pacific–Sierra Nevada motion. Normal stresses are calculated to rise at restraining bends. Measurements on rocks associated with the Hayward fault zone indicate that they have sufficient strength to support large differential stresses. If the crust surrounding faults can absorb long-term elastic strain, these results suggest that the Hayward and San Andreas faults would appear nearly frictionless in places, and strong in others, commensurate with observations.

ACKNOWLEDGMENTS

Bob Simpson and Wayne Thatcher reviewed an early version of this paper; I also benefited from discussions with George Thompson. Subsequent thoughtful suggestions by Frederick Chester and an anonymous reviewer brought many new things to my attention.

REFERENCES CITED

Bird, P., and Kong, X., 1994, Computer simulations of California tectonics confirm very low strength of major faults: Geological Society of America Bulletin, v. 106, p. 159–174.
Brocher, T.M., McCarthy, J., Hart, P.E., Holbrook, W.S., Furlong, K.P., McEvilly, T.V., Hole, J.A., and Klemperer, S.L., 1994, Seismic evidence for a possible lower-crustal detachment beneath San Francisco Bay, California: Science, v. 265, p. 1436–1439.
Brune, J.N., Henyey, T., and Roy, R.F., 1969, Heat flow, stress, and the rate of slip along the San Andreas fault, California: Journal of Geophysical Research, v. 74, p. 3821–3827.
Byerlee, J.D., 1978, Friction of rocks: Pure and Applied Geophysics, v. 116, p. 615–626.
Byerlee, J.D., 1990, Friction, overpressure and fault normal compression: Geophysical Research Letters, v. 17, p. 2109–2112.
Caristan, Y., 1982, The transition from high temperature creep to fracture in Maryland diabase: Journal of Geophysical Research, v. 87, p. 6781–6790.
Carter, N.L., and Tsenn, M.C., 1987, Flow properties of the lithosphere: Tectonophysics, v. 136, p. 27–63.
Chester, F.M., and Chester, J.S., 2000, Stress and deformation along wavy frictional faults: Journal of Geophysical Research, v. 105, p. 23,421–23,430.
Chester, F.M., Evans, J.P., and Biegel, R.L., 1993, Internal structure and weakening mechanisms of the San Andreas fault: Journal of Geophysical Research, v. 98, p. 771–786.
De Mets, C., Gordon, R.G., Argus, D.F., and Stein, S., 1994, Effect of recent revisions to the geomagnetic reversal time scale on estimates of current plate motions: Geophysical Research Letters, v. 21, p. 2191–2194.
Geist, E.L., and Andrews, D.J., 2000, Slip rates on San Francisco Bay area faults from anelastic deformation of the continental lithosphere: Journal of Geophysical Research, v. 105, p. 25,543–25,552.
Hansen, F.D., and Carter, N.L., 1983, Semibrittle creep of dry and wet Westerly granite at 1000 MPa, *in* Mathewson, C.C., ed., Proceedings of the 24th U.S. Symposium on Rock Mechanics; Theory, experiment, practice: College Station, Texas, Texas A&M University, p. 429–447.
Harris, R.A., 1998, Introduction to special section: Stress triggers, stress shadows, and implications for seismic hazard: Journal of Geophysical Research, v. 103, p. 24,347–24,358.
Henstock, T.J., Levander, A., and Hole, J.A., 1997, Deformation in the lower crust of the San Andreas fault system in northern California: Science, v. 278, p. 650–653.
Holbrook, W.S., Brocher, T.M., ten Brink, U.S., and Hole, J.A., 1996, Crustal structure beneath the San Francisco Bay block and the central California margin: Journal of Geophysical Research, v. 101, p. 22,311–22,334.
Hole, J.A., Brocher, T.M., Klemperer, S.L., Parsons, T., Benz, H.M., and Furlong, K.P., 2000, Three-dimensional seismic velocity structure of the San Francisco Bay area: Journal of Geophysical Research, v. 105, p. 13,859–13,874.
Kirby, S.H., and Kronenberg, A.K., 1987, Rheology of the lithosphere: Selected topics: Reviews of Geophysics, v. 25, p. 1219–1244.
Lachenbruch, A.H., and Morgan, P., 1990, Continental extension, magmatism, and elevation: Formal relations and rules of thumb: Tectonophysics, v. 174, p. 39–62.
Lachenbruch, A.H., and Sass, J.H., 1980, Heat flow and energetics of the San Andreas fault zone: Journal of Geophysical Research, v. 85, p. 6185–6222.
Lockner, D.A., and Byerlee, J.D., 1993, How geometrical constraints contribute to the weakness of mature faults: Nature, v. 363, p. 250–252.
Lockner, D.A., and Byerlee, J.D., 1995, An earthquake instability model based on faults containing high fluid-pressure compartments: Pure and Applied Geophysics, v. 145, p. 717–745.
Marone, C., Raleigh, C.B., and Scholz, C.H., 1990, Frictional behavior and constitutive modeling of simulated fault gouge: Journal of Geophysical Research, v. 95, p. 7007–7025.
Miller, S.A., Nur, A., and Olgaard, D.L., 1996, Earthquakes as a coupled shear stress-high pore pressure dynamical system: Geophysical Research Letters, v. 23, p. 197–200.
Moore, D.E., Lockner, D.A., Summers, R., Shengli, M., and Byerlee, J.D., 1996, Strength of chrysotile-serpentinite gouge under hydrothermal conditions: Can it explain a weak San Andreas fault?: Geology, v. 24, p. 1041–1044.
Morrow, C.A., and Lockner, D.A., 2001, Hayward fault rocks: Porosity, density and strength measurements: U.S. Geological Survey Open-File Report, v. 01–421, 28 p.
Parsons, T., 2002, Post-1906 stress recovery of the San Andreas fault system calculated from 3-D finite element modeling: Journal of Geophysical Research (in press).
Parsons, T., and Hart, P.E., 1999, Dipping San Andreas and Hayward faults revealed beneath San Francisco Bay, California: Geology, v. 27, p. 839–842.
Reasenberg, P.A., and Simpson, R.W., 1992, Response of regional seismicity to the static stress change produced by the Loma Prieta earthquake: Science, v. 255, p. 1687–1690.
Rice, J.R., 1992, Fault stress states, pore pressure distributions, and the weakness of the San Andreas Fault, *in* Evans, B., and Wong, T. eds., Fault mechanics and transport properties of rocks; a festschrift in honor of W. F. Brace: San Diego, California, Academic Press, p. 475–503.
Saffer, D.M., Frye, K.M., Marone, C., and Mair, K., 2001, Laboratory results indicating complex and potentially unstable frictional behavior of smectite clay: Geophysical Research Letters, v. 28, p. 2297–2300.
Saucier, F., Humphreys, E., and Weldon, R., II, 1992, Stress near geometrically complex strike-slip faults: Application to the San Andreas fault at Cajon Pass, southern California: Journal of Geophysical Research, v. 97, p. 5081–5094.
Savage, J.C., Svarc, J.L., and Prescott, W.H., 1999, Geodetic estimates of fault slip rates in the San Francisco Bay area: Journal of Geophysical Research, v. 104, p. 4995–5002.
Scholz, C.H., 1996, Faults without friction?: Nature, v. 381, p. 556–557.
Scholz, C.H., 2000, Evidence for a strong San Andreas fault: Geology, v. 28, p. 163–166.
Sibson, R.H., 1994, An assessment of field evidence for ‘Byerlee’ friction: Pure and Applied Geophysics, v. 142, p. 645–662.
Sleep, N.H., and Blanpied, M.L., 1992, Creep, compaction and the weak rheology of major faults: Nature, v. 359, p. 687–692.
Wintsch, R.P., Christoffersen, R., and Kronenberg, A.K., 1995, Fluid-rock reaction weakening of fault zones: Journal of Geophysical Research, v. 100, p. 13,021–13,032.
Zoback, M.D., 2000, Strength of the San Andreas: Nature, v. 405, p. 31–32.
Zoback, M.D., Zoback, M.L., Mount, V.S., Suppe, J., Eaton, J.P., Healy, J.H., Oppenheimer, D.H., Reasenberg, P.A., Jones, L.M., Raleigh, C.B., Wong, I.G., Scotti, O., and Wentworth, C.M., 1987, New evidence of the state of stress of the San Andreas fault system: Science, v. 238, p. 1105–1111.

Manuscript received April 18, 2002
Revised manuscript received August 15, 2002
Manuscript accepted August 20, 2002

Printed in USA